Soil Dynamics and Earthquake Engineering 136 (2020) 106118

Contents lists available at ScienceDirect

Soil Dynamics and Earthquake Engineering

journal homepage: http://www.elsevier.com/locate/soildyn

Study on seismic behaviors of a double box utility tunnel with joint connections using shaking table model tests

Wengang Zhang [a,b,c], Liang Han [b], Li Feng [b], Xuanming Ding [a,b,c], Lin Wang [b], Zhixiong Chen [b], Hanlong Liu [a,b,c,*], Ashraf Aljarmouzi [b], Weixin Sun [d]

[a] Key Laboratory of New Technology for Construction of Cities in Mountain Area, Chongqing University, Chongqing, China
[b] School of Civil Engineering, Chongqing University, Chongqing, China
[c] National Joint Engineering Research Center of Geohazards Prevention in the Reservoir Areas, Chongqing University, Chongqing, China
[d] Department of Infrastructure Engineering, Melbourne School of Engineering, The University of Melbourne, VIC, 3010, Australia

ARTICLE INFO

Keywords:
Double box utility tunnel
Joint connection
Shaking table test
Seismic behaviors

ABSTRACT

Shaking table model tests were carried out to study the seismic behaviors of double box utility tunnel with joint connections and the surrounding soil. The seismic wave obtained from 1952 Taft earthquake was employed as the input in this study, and its PGA has been adjusted to 0.2 g, 0.4 g, 0.8 g, and 1.2 g, respectively. In addition, a series of sine waves with PGA of 0.2 g and frequencies of 5 Hz, 10 Hz, 15 Hz, 20 Hz, 25 Hz, and 30 Hz were applied to study the effect of frequency characteristics on seismic behavior of the utility tunnel and the surrounding soil. The testing results show that the laminar soil container does not impose significant boundary effect, and the dynamic earth pressure response is significantly influenced due to existence of the joint connection. Besides, the effect of soil-structure interaction on seismic behaviors is becoming even more obvious as the input PGA increases. The acceleration response is also significantly influenced by the dynamic property of the soil. Greater bending moment occurs at the corners of the structure, and its increasing ratio will decrease with an increasing input PGA magnitude. Lastly, the effect of frequency is significant. Therefore, it is noteworthy that the possible effect of natural frequency is considered when the utility tunnel is under construction.

1. Introduction

The role of underground lifelines (like water pipe, gas pipe, and electric wire) is drawing increasing attention in modern developed societies where living conditions, the economic, cultural and social activities are increasingly dependent on a complex network of lifelines [1]. How to maintain the operation of these lifelines, as well as the ensurance of safety, becomes a key issue. Nowadays, underground utility tunnel, an emerging infrastructure, is gradually applied for development of city due to it is multifunctional and maintenance-friendly [2]. Despite that the seismic performance of underground structure has been paid attention since the 1995 Kobe-Osaka earthquake [3,4], the study on seismic behavior of underground utility tunnel is not systematic and enough. The research results of seismic behavior about other underground structures are not suitable for application of the underground utility tunnel, because it has some extinct features, like relatively small cross section, shallowly buried, and relatively simple structure pattern. Since many pipelines for water, electricity, and natural gas, etc. will be put into it, the consequences are unimaginable once earthquake occurs. Therefore, it is essential to conduct the research on seismic behavior of underground utility tunnel and the surrounding soil.

From the aspect of seismic behavior research of underground structure, many researchers have made great efforts and achieved a lot of achievements. Martin and Seed [5] have studied the difference of analysis result for the seismic response of a layered site between equivalent linear and non-linear methods. Gil et al. [6] proposed an alternative method to approximate the seismic stresses of a buried reinforced concrete structure, while this method is suitable for site subjected to compressive wave. Hashash et al. [7] thoroughly summarized the current state of seismic analysis and design for underground structure, and the authors also presented several special design issues including the design of joint connections in tunnel engineering. Hashash et al. [8] made a comparison between two analytical solutions for estimating the ovaling deformation and forces in circular tunnels due to soil–structure interaction under seismic effect. Tateishi [9] proposed a new method of seismic load application and verifies the validity through

* Corresponding author. Key Laboratory of New Technology for Construction of Cities in Mountain Area, Chongqing University, Chongqing, China.
E-mail address: hliuhhu@163.com (H. Liu).

https://doi.org/10.1016/j.soildyn.2020.106118
Received 27 September 2019; Received in revised form 9 February 2020; Accepted 1 March 2020
Available online 23 May 2020

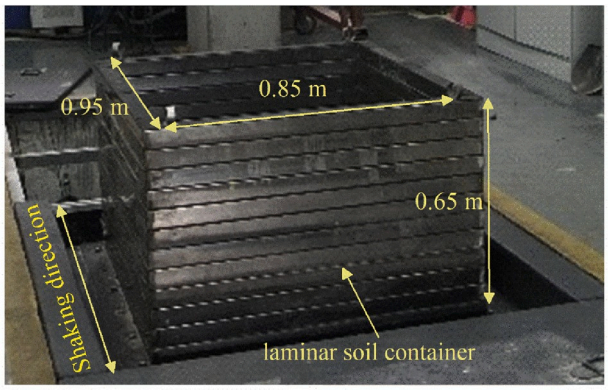

Fig. 1. Shaking table test system.

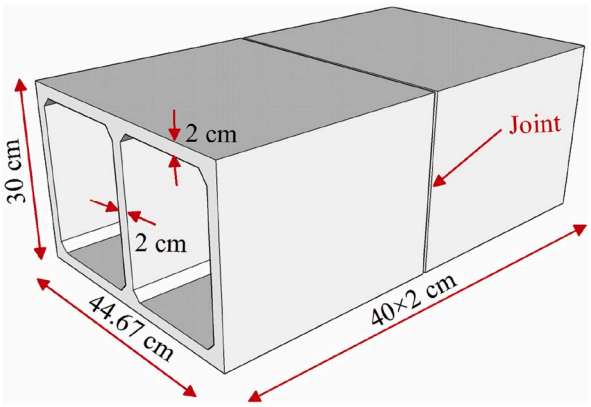

Fig. 2. Schematic plot of double box utility tunnel model with joint connections.

Table 1
Similarity ratios for parameters chosen.

	Calculation	Similarity ratio
Geometry S_l	Selected	1:15
Strain S_ε	Selected	1:1
Stress S_σ	Selected	1:3
Elastic modulus S_E	$S_E = S_\sigma/S_\varepsilon$	1:3
Acceleration S_a	Selected	5:1
Density S_ρ	$S_\rho = S_E/(S_l \cdot S_a)$	1:1
Time S_t	$S_t = \sqrt{Sl/Sa}$	1:8.67
Reinforcement	Keep the reinforcement ratio is consistent with the actual project	

numerical analyses of the underground duct. However, he assumed that response accelerations of the structure and the near-field are the same as those of the free field at the same location, which remains to be experimentally verified. With the improvement of testing equipment and computational capacity, a series of new research means have been introduced into the earthquake engineering research. For instance, geotechnical centrifuge experiments have been applied for the research of seismic behavior of soil–foundation–structure interaction [10]. Wang et al. [11] conducted a shaking table model test to explore the seismic response of underground tunnel-soil-surface structure interaction system. A multi-point shaking table test of a long tunnel subjected to non-uniform seismic loadings was carried out by Yu et al. [12], where the acceleration response of the tunnel and the tunnel joints deformation was investigated. For utility tunnel, Jiang et al. and Chen et al. [13,14] have applied the shaking table test and numerical simulation to investigate the seismic response of the structure and the surrounding soil. By means of shaking table test, Yan et al. [15] and Chen et al. [16] studied the influence of non-uniform excitation on seismic performances of a utility tunnel. In the research above, the single box utility tunnel without joint was considered only, which has a certain gap with the actual project.

Based on the researches mentioned above, this study conducted a shaking table model test for the double box utility tunnel with a joint connection. Firstly, based on the similarity theory, a scaled double box utility tunnel with a joint connection was designed. Then, a true seismic wave and a series of sine wave with different frequencies were employed to investigate the seismic behavior of structure and the surrounding soil and the effect of frequency on seismic performance, respectively.

2. Testing design and instruments

The tests were conducted via a shaking table test system developed by ANCO Company in Geotechnical Laboratory Center of Chongqing University (see Fig. 1). This shaking table test system can sustain a peak acceleration which is not more than 1.2 g and a frequency of seismic

Fig. 3. Instrumentation and the joint location.

wave ranging from 0 to 50 Hz. During the test, a laminar shearing steel soil container with the dimension of 0.95 × 0.85 × 0.65 m (length × width × height) was applied to eliminate boundary effect.

Based on Lai [17], the similarity ratios for physical and mechanical properties and time parameters of the test model are designed as illustrated in Table 1. Considering the test equipment condition, the similarity ratios of geometry, strain, and stress was directly selected. Since the maximum vibration acceleration of this shaking table is 1.2g, the original acceleration in actual project is about 0.25 g with Sa = 5. Therefore, adopting this acceleration similarity ratio (Sa = 5), the

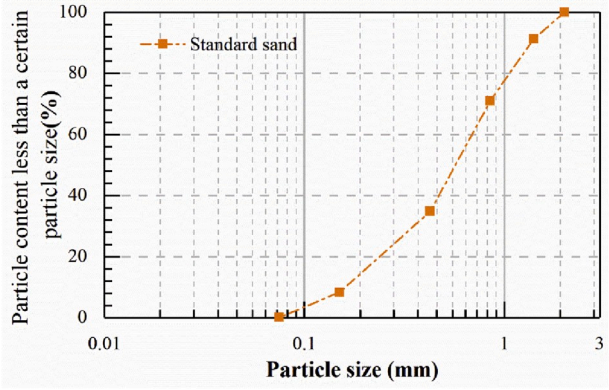

Fig. 4. Grain size distribution curve of the standard sand [28].

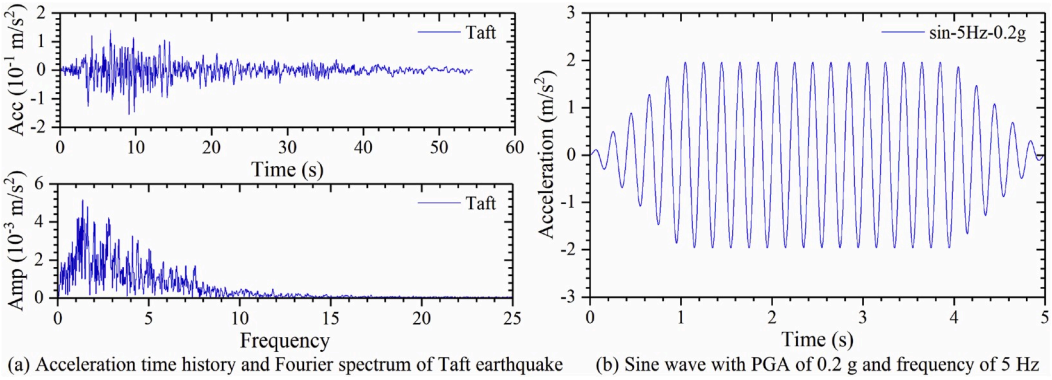

Fig. 5. Input seismic spectrum in this study.

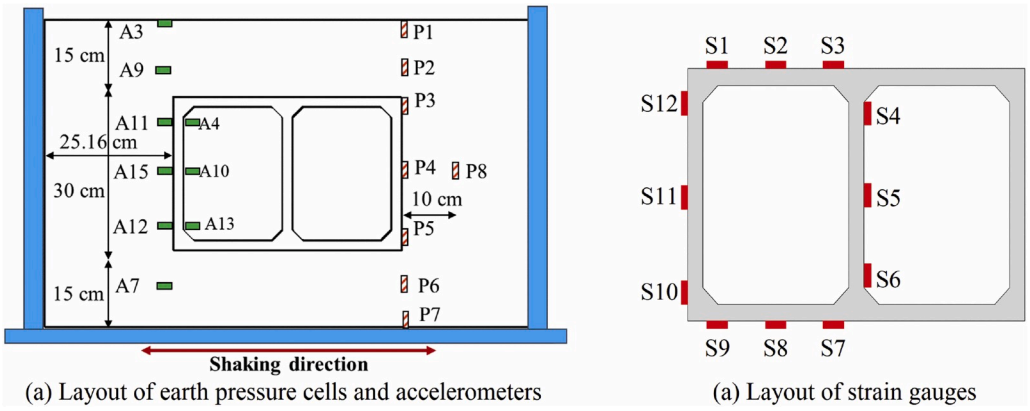

Fig. 6. Layout of earth pressure meters and accelerometers at the joint cross-section.

performance of this shaking table can be fully utilized.

Based on Table 1, the utility tunnel model is made of micro-concrete which is similar to concrete with the elastic modulus of 6062 MPa with two sections which contacted each other directly (see Fig. 2). Galvanized iron wire is used to simulate the reinforcement. Fig. 3 shows the diagram of testing model, and it can be seen that the joint was covered by HDPE

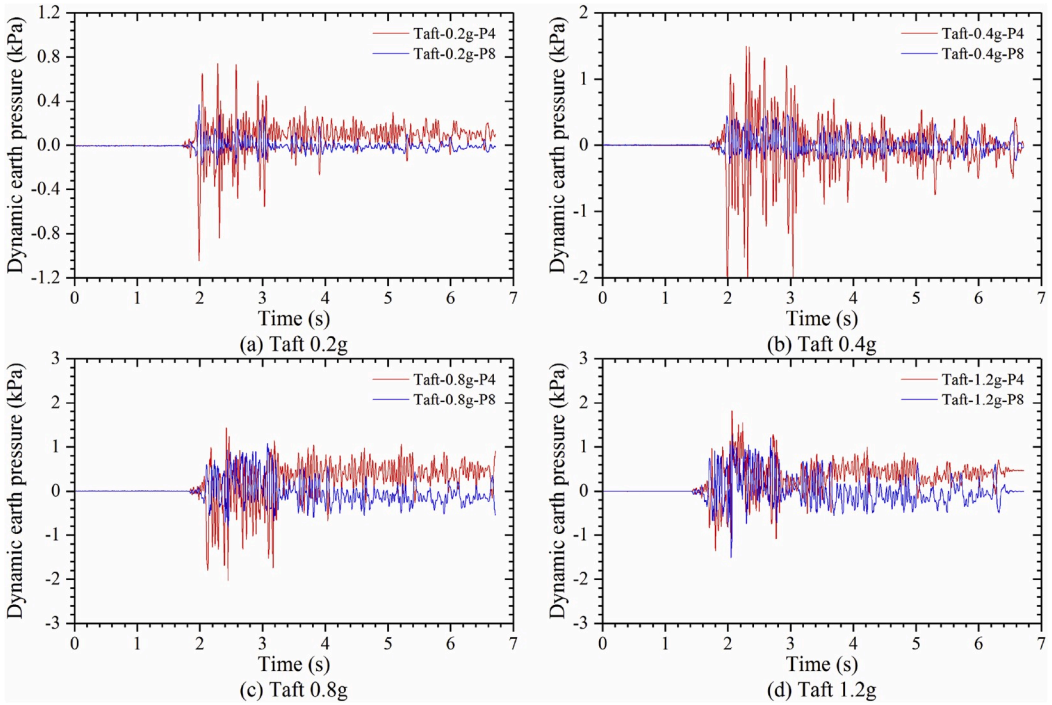

Fig. 7. Time history of dynamic earth pressure responses of P4 and P8 for various input PGAs.

black geomembrane with thickness of 0.2 mm, which indicates that this joint connection can be regarded as a kind of flexible connection. The standard sand in Fujian province was used to simulate the sand field and its grain size distribution curve was shown in Fig. 4. After the layered compaction treatment in the test, the simulated sand field density is approximately 1740 kg/m^3.

In this study, the seismic wave of 1952 Taft earthquake with the duration of 54 s and the peak ground acceleration (PGA) of 0.014 g was selected as the input seismic wave and its original acceleration time history and Fourier spectrum are shown in Fig. 5 (a). To examine the effect of PGA on seismic behavior of structure and the surrounding soil, Taft seismic spectrum has been adjusted to have the PGA of 0.2 g, 0.4 g, 0.8 g, and 1.2 g, respectively. Besides, a series of sine waves with input PGA of 0.2 g and frequency of 5 Hz, 10 Hz, 15 Hz, 20 Hz, 25 Hz, and 30 Hz were employed to investigate the effect of frequency on seismic behaviors of structure and the surrounding soil. Fig. 5 (b) shows the input sine wave with PGA of 0.2 g and frequency of 5 Hz, and other sine wave spectrum is similar with that.

Considering the symmetry of the testing model, the longitudinal axis of the utility tunnel section is the axis of symmetry, earth pressure cell and accelerometer were arranged on each side as demonstrated in Fig. 6 (a). In order to study the bending moment response law of the utility tunnel structure, a series of strain gauges are evenly arranged on the outer wall of joint cross-section of the Utility tunnel as shown in Fig. 6 (b).

3. Analysis of testing results

3.1. Boundary effect analysis

The boundary effect is an essential element for the shaking table model test, and it can directly determine the quality of testing results. Therefore, it is necessary to check the boundary effect in this study. Generally speaking, the laminar soil container can mitigate the boundary effect [18,19]. However, this soil container is relatively small than other researches [20–22], which means that the boundary may still take effect. Feng et al. (2020) has conducted shaking table tests for a single-box utility tunnel using the same shaking table system and laminar soil container, which indicates that the boundary effect can be well controlled [23]. For laminar soil container, Lee et al. (2012) has performed a comprehensive research about the boundary effect of laminar soil container using a series of shaking table tests [18]. Finally, it was concluded that the seismic responses in the tests will not be affected by the boundary if measuring point was arranged at a distance of approximately 1/20th of the model length from the end walls of laminar soil container and not positioned on the ground surface. According to the references above, the boundary effect in this study can be well mitigated.

After the review of the previous research, the seismic responses will be employed to investigate the boundary effect in this study. To this end, the time history of dynamic earth pressure responses of P4 and P8 were plotted in Fig. 7. Based on the observation, the responses of P4 and P8 are slightly consistent with each other, especially for the lower input PGA (0.2 g and 0.4 g). The Pearson correlation coefficient calculated by equation (1) was applied to analyze the consistence of dynamic earth pressure responses of the two testing points.

$$\rho_{R1,R2} = \frac{COV(R1, R2)}{\sqrt{D(R1)}\sqrt{D(R2)}} \quad (1)$$

where *R1* and *R2* are the seismic responses of reference point and testing point, respectively; COV(*R1*, *R2*) is the covariance of *R1* and *R2*; D(*R1*) and D(*R2*) are the variance of *R1* and *R2*; and $\rho_{R1,R2}$ is the correlation coefficient of *R1* and *R2*.

The closer to 1 or -1 the $\rho_{R1,R2}$ is, the more consistent the seismic responses of the two measuring points are with each other. Judged by

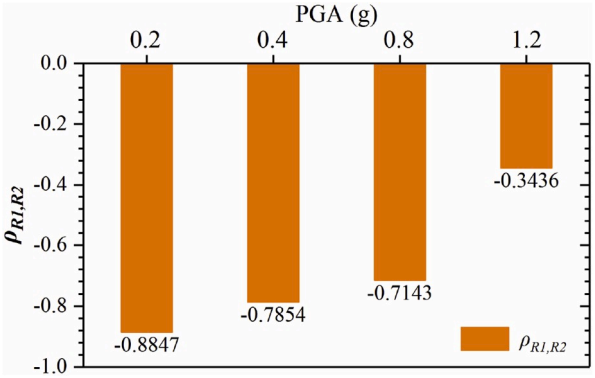

Fig. 8. Consistence testing between the seismic responses of P4 and P8.

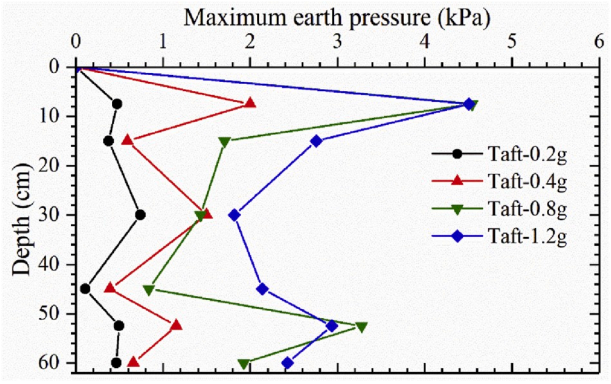

Fig. 9. Maximum earth pressure response in the soil adjacent to the side-wall.

Pearson correlation coefficient, $0<|\rho_{R1,R2}|<0.2$ means the responses are inconsistent; $0.2<|\rho_{R1,R2}|<0.4$ means slightly consistent; $0.4<|\rho_{R1,R2}|<0.6$ means moderately consistent; $0.6<|\rho_{R1,R2}|<0.8$ means strongly consistent; $0.8<|\rho_{R1,R2}|<1.0$ means highly consistent. In this study, we assumed that P4 is the reference point and P8 is the testing point. The analysis results were given in Fig. 8. Firstly, these negative values mean the dynamic soil responses for P4 and P8 are opposite, which is reasonable as the horizontal earth pressure can be larger along the direction of shaking. Then, the values of absolute values of $\rho_{R1,R2}$ of PGA = 0.2 g, 0.4 g, and 0.8 g are generally greater than 0.7 and the value of PGA = 1.2 g is 0.3436, hence the seismic responses of P4 and P8 are basically synchronous. Therefore, the analysis above further indicates that the boundary effect in this study is well controlled.

3.2. Analysis of earth pressure

As for the seismic effect and soil-structure interaction, the earth pressure has some extinct characteristic, compared with the static state. Fig. 9 shows the maximum earth pressure response in the soil adjacent to the side-wall. It is shown that the greater maximum earth pressure occurs at the position above the top of side-wall and beneath the bottom of side-wall. And the maximum earth pressure at the middle part of side-wall is greater than that at the top and bottom part of side-wall except for Taft 0.8 g and 1.2 g condition. This result is beyond the general understanding. Generally speaking, there may be a soil arch, in which case the greater maximum earth pressure will occur at the top and bottom part of the side-wall not at the middle part. Therefore, it can be concluded that the soil arch did not develop (or did not fully form) due to the existence of joint. It still can be observed that most maximum dynamic earth pressure value increases with an increasing input PGA except for the position at the middle part of the side-wall. It can be implied that the soil arch effect will be more significant with relatively

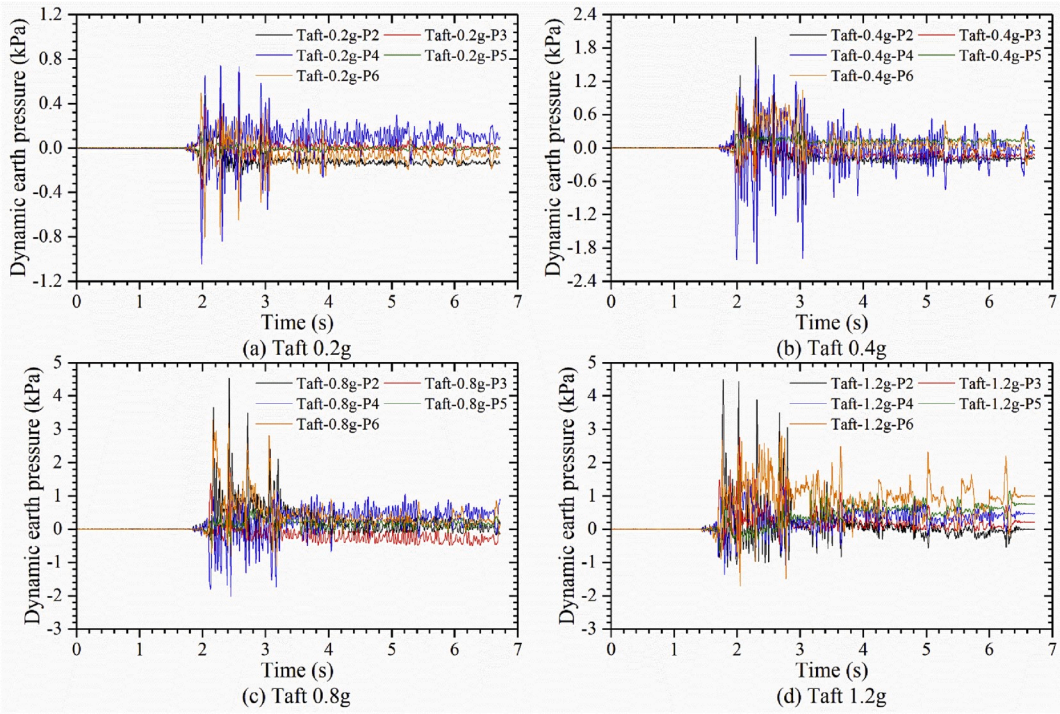

Fig. 10. Earth pressure time history in the soil adjacent to the side-wall.

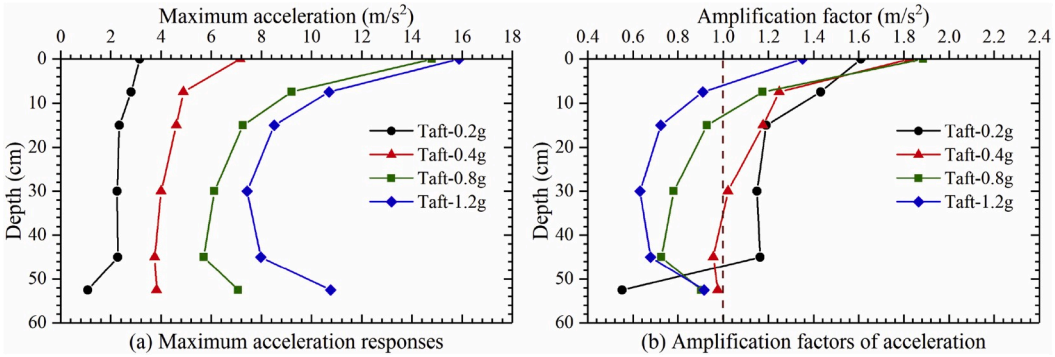

Fig. 11. Maximum acceleration responses and its amplification factors in the soil adjacent to the side-wall.

greater input PGA.

Fig. 10 shows the time history of dynamic earth pressure. Firstly, the basic law of dynamic earth pressure response for different measuring points is similar under four kinds of input PGA. Then, most of times, it can be seen that the dynamic earth pressure response of P3 and P5 is less than that of P4, suggesting that the horizontal soil arch did not fully develop due to the existence of joint. Lastly, it is clear that the earth pressure is greater or less than it under static condition at the end of earthquake, which indicates that the contact between the side-wall and the adjacent soil got weaken or strengthened in the shaking process.

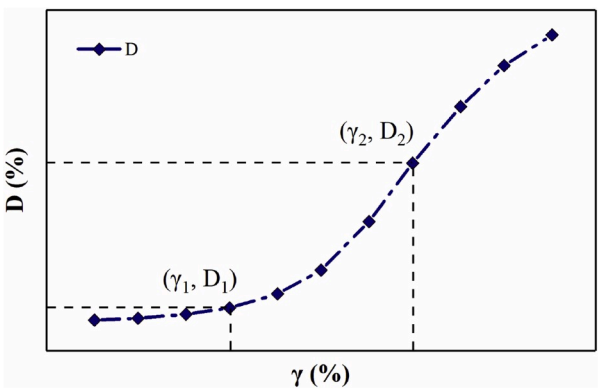

Fig. 12. Relationship between dynamic shear strain γ and damping ratio D.

3.3. Analysis of acceleration response

A series of acceleration measuring points (A3, A9, A11, A15, A12, and A7) are arranged to monitor the acceleration response in the soil adjacent to the side-wall (see Fig. 6 (a)). The result of testing shows that the maximum acceleration response will increase with an increasing input PGA at a specific depth (see Fig. 11). On the whole, it can be seen that the maximum acceleration response decreases with the increasing depth. However, when the input PGA is 0.8 g and 1.2 g, it is clearly observed that the maximum acceleration slightly increases from the bottom of the side-wall to the measuring point A7, which suggests that the effect of underground structure on seismic performance of soil will get greater as the input PGA increases.

Amplification factor is a suitable indicator reflecting the seismic

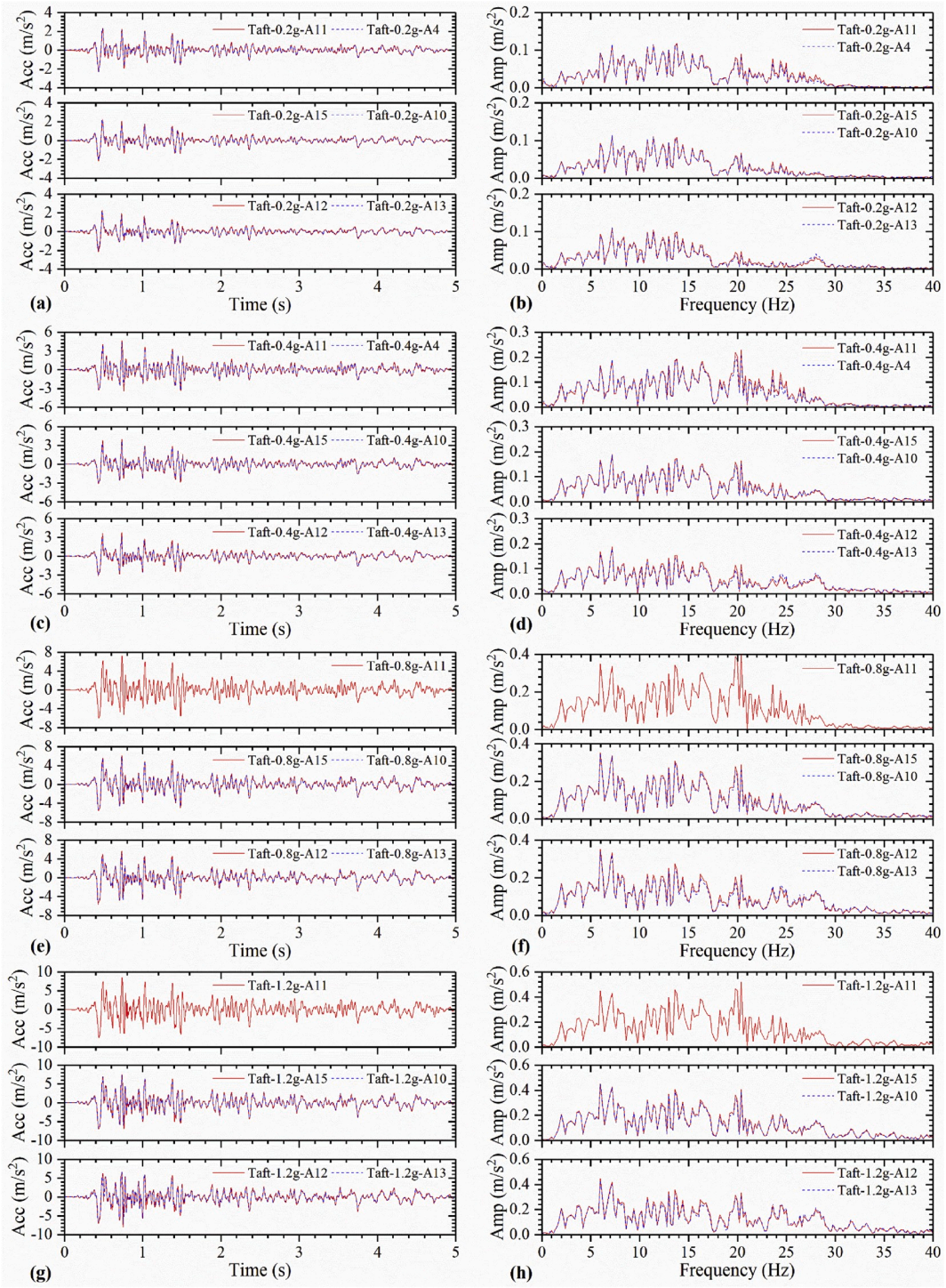

Fig. 13. Comparison of acceleration time history ((a) Taft 0.2 g, (c) Taft 0.4 g, (e) Taft 0.8 g, and (g) Taft 1.2 g) and Fourier spectrum ((b) Taft 0.2 g, (d) Taft 0.4 g, (f) Taft 0.8 g, and (h) Taft 1.2 g) for the measuring points in the soil and structure at the same depth.

performance of site. The greater the value is, the more significance the seismic response is of. It is obvious that the value will decrease with depth and decrease as input PGA increases (see Fig. 11 (b)). Besides, most amplification factors under 0.2 g and 0.4 g are greater than 1.0, whereas it is opposite to condition of 0.8 g and 1.2 g, indicating the degree of amplification will diminish with an increasing input PGA. The phenomenon above which is consistent with the research of Jiang et al. [13] and Chen et al. [24] may result from the dynamic damping of soil (see Fig. 12). Firstly, the seismic wave with greater input PGA will render shearing strain increase from γ_1 to γ_2, and the corresponding damping ratio will increase from D1 to D_2 so that the true maximum acceleration response of site will be smaller and smaller and evenly less than the input PGA.

The effect of underground structure on seismic performance of soil has been observed (see Fig. 11 (a)). And in this part, the soil-structure interaction is further illustrated with the monitor data of measuring points (A11, A4, A15, A10, A12 and A13) (see Fig. 13). The accelerometer of measuring point A4 was broken during the test so that the acceleration data of A4 cannot be obtained under Taft 0.8 g and 1.2 g condition. According to the acceleration time history and the

Table 2
Bending moments at different strain measuring points.

	Taft - 0.2 g	Taft - 0.4 g	Taft - 0.8 g	Taft -1.2 g
S1	5.41	11.21	20.26	23.93
S2	0.86	1.43	2.55	2.25
S3	−3.90	−9.92	−20.34	−22.69
S4	−5.12	−9.78	−18.85	−21.91
S5	−1.66	−3.46	−7.47	−8.38
S6	7.53	13.81	23.63	27.75
S7	4.35	8.28	16.04	18.66
S8	−0.98	−2.37	−6.26	−7.88
S9	−6.58	−12.12	−23.95	−28.96
S10	−4.91	−9.23	−17.08	−20.05
S11	0.22	−0.30	0.82	1.80
S12	5.21	10.37	19.18	22.67

corresponding Fourier spectrum, it still can be seen that the acceleration response in the soil adjacent to the side-wall matches very well with it on the side-wall of the structure (see Fig. 13), which suggests that the soil adjacent to the side-wall has the similar motion pattern with structure and they did not separate with each other during the earthquake process. This conclusion is useful for the establishment of the calculation theory. Additionally, the frequency ingredient in these acceleration response mainly ranges from 1 Hz to 30 Hz, which is within the allowable scope (0–50 Hz) of this shaking table system, indicating the test result is reliable. The acceleration response at the same time increases with an increasing PGA in acceleration time history as demonstrated in Fig. 13 (a), (c), (e), and (g), as well as the amplitude at the same frequency has the similar law in Fourier spectrum as demonstrated in Fig. 13 (b), (d), (f), and (b).

3.4. Analysis of structure moment response

According to the above analysis, it can be seen that the difference of seismic response is significant along depth especially for the dynamic earth pressure response. Based on the dynamic strain responses, the time of greatest strain response will be firstly determined. Then, the strain response of each measuring point at that time was employed to calculate the bending moment using equation (2):

$$M = \varepsilon \cdot W \cdot E \cdot 10^{-9} \tag{2}$$

where M is the bending moment of structure per unit length, N m/m; ε is the strain response, 10^{-6}; W is the section modulus in bending, mm^3; E is the elastic modulus of the micro-concrete, MPa.

The bending moments at the strain measuring points (S1 ~ S12) have been calculated as listed in Table 2. It is shown that the bending moment of structure displays an extinct distribution (see Fig. 14) under the effect of force and motion. It can be clearly seen that the bending moment response has an antisymmetric distribution, where the greater bending moment response occurred at the corners of the structure, whereas the bending moment responses at the middle part of each side-wall are far less than that at the corners. It suggests that the twist distortion exists for utility tunnel under earthquake condition.

As input PGA increases, the bending moment response also become greater at the corresponding measuring point. Therefore, during the construction of underground utility tunnel, the strength of corner should be paid more attention than any part under static stage considering the seismic effect. However, as shown in Table 3, the increasing ratio of bending moment (IROBM) at corners decreases as the input PGA increases, indicating that the whole utility tunnel was moving with

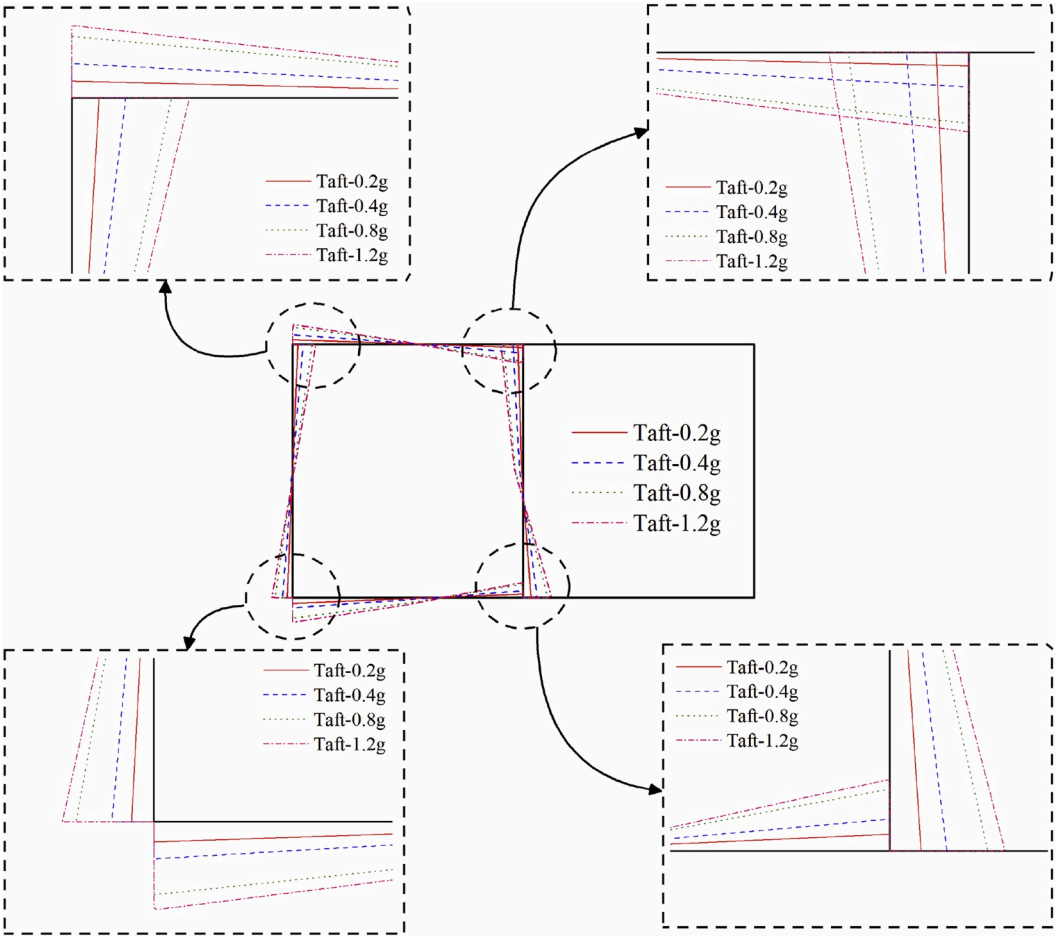

Fig. 14. Bending moment response of utility tunnel model.

Table 3
IROBM value at the corners under four kinds of input PGA conditions (%).

	0.2g–0.4 g	0.4g–0.8 g	0.8g–1.2 g
S1	107.44	40.36	18.11
S3	154.50	52.52	11.57
S4	90.87	46.37	16.24
S6	83.39	35.56	17.46
S7	90.10	46.90	16.34
S9	84.32	48.78	20.92
S10	88.10	42.53	17.41
S12	99.13	42.42	18.24

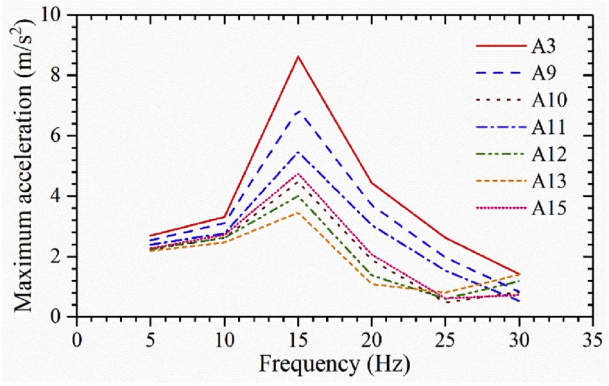

Fig. 15. Maximum acceleration response under the sine wave with various frequencies.

relatively slight twist distortion under relatively greater input PGA. IROBM is calculated using equation (3). In actual project, if that case occurs, the failure mainly develops along its longitudinal direction, i.e., the utility tunnel may get damaged at some place along its longitudinal direction.

$$IROBM = \frac{BM_2 - BM_1}{BM_1} \times \frac{0.2g}{PGA_2 - PGA_1} \tag{3}$$

where PGA_1 and PGA_2 are the previous input PGA and the latter input PGA during the shaking table test, respectively; the BM_1 and BM_2 are the bending moment values at the same position of the structure under the earthquake with PGA_1 and PGA_2 respectively.

3.5. Effect of shaking wave frequency on seismic performance

Previous studies have revealed that the frequency ingredient of seismic wave plays a significant role in the seismic performance of structure [25,26]. For actual seismic wave, it consists of a wide range of frequency ingredient without regulation so that it is hard to investigate the effect of frequency property on seismic performance. Therefore, the sine wave is taken into consideration with different frequencies, Tamari and Towhata [27] also applied sine wave to conduct the similar research. To make full use of the performance of shaking table test, six sine waves with the input PGA of 0.2 g were chosen and frequency is 5 Hz, 10 Hz, 15 Hz, 20 Hz, 25 Hz, and 30 Hz, respectively. The maximum seismic responses were extracted from the observed data of those measuring points to analysis the possible natural frequency for this whole system.

Fig. 15, Fig. 16, and Fig. 17 show the maximum acceleration response, the maximum dynamic earth pressure response, and the maximum strain response under sine wave with various frequencies. From the three figures above, it can be seen that the greater maximum responses of the ground and the structure all occurred when the frequency is 15 Hz for each measuring point, showing that the natural frequency may be around 15 Hz for this soil-understructure system.

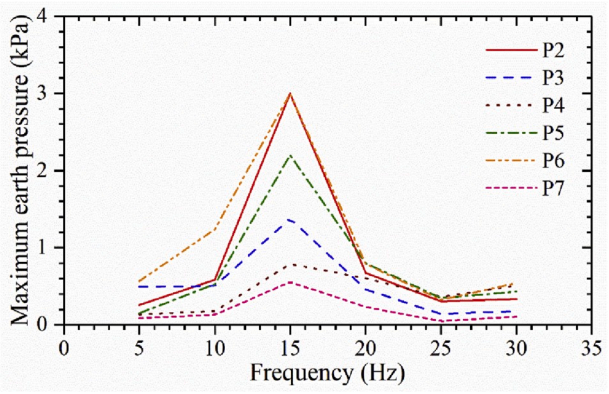

Fig. 16. Maximum dynamic earth pressure response under the sine wave with various frequencies.

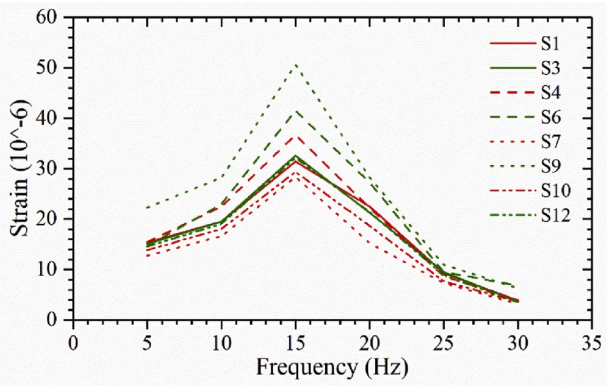

Fig. 17. Maximum strain response under the sine wave with various frequencies.

Even through the input PGA is the same, the seismic response under natural frequency is significant greater than that under other frequency. Hence, taking the natural frequency into consideration is essential during the construction of underground structure.

4. Summary and conclusions

By means of shaking table model tests, the seismic behaviors of double box utility tunnel with joint connections as well as the surrounding soil are studied. The following conclusions are drawn:

(1) Through the evaluation by Person correlation coefficient, the boundary effect is related to input PGA. The greater input PGA will impose the more significant boundary effect. Most of the absolute values of $\rho_{R1,R2}$ are greater 0.7, which demonstrates that the laminar soil container used in this test does not bring in significant boundary effect.
(2) According to the maximum acceleration response, it is found that the effect of soil-structure interaction on seismic behavior is growing significant as input PGA increases. And the amplification factor become smaller with an increasing input PGA, which may be due to the effect of the relationship of dynamic shear strain and damping ratio. The soil adjacent to the side-wall keeps the motion that is consistent with the structure, which is useful for the research of calculation theory.
(3) Due to the existing of a joint connection, the horizontal soil arch does not fully form so that the maximum earth pressure at the middle of the side-wall is greater than it at the top and bottom of the side-wall.

(4) For the bending moment of the structure, the greater bending moment will occur at the corners of the structure, and its increasing ratio become smaller as input PGA increases, in which case the failure of utility tunnel is mostly likely to take place along the longitudinal direction, not the cross-section.
(5) The effect of frequency is greatly significant, and the natural frequency 15 Hz was determined since the seismic response under this frequency remains significantly greater than it under other frequencies. Therefore, it is worth considering the possible effect of natural frequency when the underground structure is under construction.

Declaration of competing interest

The authors declare that they have no known competing financial interests or personal relationships that could have appeared to influence the work reported in this paper.

Acknowledgments

The project was supported by the Chongqing Construction Science and Technology Plan Project (2019-0045), Natural Science Foundation of Chongqing, China (cstc2018jcyjAX0632), and Graduate Research and Innovation Foundation of Chongqing, China (Grant No. CYS18021).

Appendix A. Supplementary data

Supplementary data to this article can be found online at https://doi.org/10.1016/j.soildyn.2020.106118.

References

[1] Pitilakis K, Alexoudi M, Argyroudis S, Monge O, Martin C. Earthquake risk assessment of lifelines. Bull Earthq Eng 2006;4(4):365–90.
[2] Hu CP, Zhang SL. Study on BIM Technology application in the whole life cycle of the utility tunnel. In: Zeng X, et al., editors. International symposium for intelligent transportation and smart city (ITASC) 2019 proceedings. Singapore: Springer Nature Singapore Pte Ltd.; 2019. p. 277–85.
[3] Patil M, Choudhury D, Ranjith PG, Zhao J. Behavior of shallow tunnel in soft soil under seismic conditions. Tunn Undergr Space Technol 2018;82:30–8.
[4] Ma C, Lu DC, Du XL, Qi CZ. Effect of buried depth on seismic response of rectangular underground structures considering the influence of ground loss. Soil Dynam Earthq Eng 2018;106:278–97.
[5] Martin PP, Seed HB. One-dimensional dynamic ground response analyses. J Geotech Eng Div ASCE 1982;108(7):935–52.
[6] Gil LM, Hernandez E, De la Fuente P. Simplified transverse seismic analysis of buried structures. Soil Dynam Earthq Eng 2001;21:735–40.
[7] Hashash YMA, Hook JJ, Schmidt B, Yao JIC. Seismic design and analysis of underground structures. Tunn Undergr Space Technol 2001;16:247–93.
[8] Hashash YMA, Park D, Yao JIC. Ovaling deformations of circular tunnels under seismic loading, an update on seismic design and analysis of underground structures. Tunn Undergr Space Technol 2005;20:435–41.
[9] Tateishi A. A study on seismic analysis methods in the cross section of underground structures using static finite element method. Struct Eng 2005;22(1):41s–54s.
[10] Mason HB, Trombetta NW, Chen Z, Bray JD, Hutchinson TC, Kutter BL. Seismic soil–foundation–structure interaction observed in geotechnical centrifuge experiments. Soil Dynam Earthq Eng 2013;48:162–74.
[11] Wang GB, Yuan MZ, Miao Y, Wu J, Wang YX. Experimental study on seismic response of underground tunnel-soil-surface structure interaction system. Tunn Undergr Space Technol 2018;76:145–59.
[12] Yu HT, Yan X, Bobet A, Yuan Y, Xu GP, Su QK. Multi-point shaking table test of a long tunnel subjected to non-uniform seismic loadings. Bull. Earthq Eng 2017;16(2):1041–59.
[13] Jiang LZ, Chen J, Li J. Seismic response of underground utility tunnels: shaking table testing and FEM analysis. Earthq Eng Eng Vib 2010;9(4):555–67. https://doi.org/10.1007/s11803-010-0037-x.
[14] Chen J, Shi XJ, Li J. Shaking table test of utility tunnel under non-uniform earthquake wave excitation. Soil Dynam Earthq Eng 2010;30(11):1400–16.
[15] Yan KM, Zhang JJ, Wang ZJ, Liao WM, Wu ZJ. Seismic responses of deep buried pipeline under non-uniform excitations from large scale shaking table test. Soil Dynam Earthq Eng 2018;113:180–92.
[16] Chen ZY, Liang SB, He C. Effects of different coherency models on utility tunnel through shaking table test. J Earthq Eng 2018:1–22.
[17] Iai S. Similitude for shaking table tests on soil-structure-fluid model in 1g gravitational field, soils and foundations. Soils Found 1989;29(1):105–18.
[18] Lee CJ, Wei YC, Kuo YC. Boundary effects of a laminar container in centrifuge shaking table tests. Soil Dynam Earthq Eng 2012;34:37–51.
[19] Duan X, Dong Q, Ye WJ. Experimental study on seismic performance of prefabricated utility tunnel. Adv Civ Eng 2019:1–14. https://doi.org/10.1155/2019/8968260. 2019, Article ID: 8968260.
[20] Zhuang HY, Wang X, Miao Y, Yao EL, Chen S, Ruan B, et al. Seismic responses of a subway station and tunnel in a slightly inclined liquefiable ground through shaking table test. Soil Dynam Earthq Eng 2019;116:371–85.
[21] Zhang JH, Yuan Y, Yu HT. Shaking table tests on discrepant responses of shaft-tunnel junction in soft soil under transverse excitations. Soil Dynam Earthq Eng 2019;120:345–59.
[22] Zhao HL, Yuan Y, Ye ZM, Yu HT, Zhang ZM. Response characteristics of an atrium subway station subjected to bidirectional ground shaking. Soil Dynam Earthq Eng 2019;125. https://doi.org/10.1016/j.soildyn.2019.105737.
[23] Feng L, Ding XM, Wang CL, Chen ZX. Shaking table model test on seismic responses of utility tunnel with joint. Rock and Soil Mechanics; 2020. p. 1–10. https://doi.org/10.16285/j.rsm.2019.0857 (In Chinese) (Online).
[24] Chen GX, Chen S, Zuo X, Du XL, Qi CZ, Wang ZH. Shaking-table tests and numerical simulations on a subway structure in soft soil. Soil Dynam Earthq Eng 2015;76:13–28.
[25] Cakir T. Evaluation of the effect of earthquake frequency content on seismic behavior of cantilever retaining wall including soil–structure interaction. Soil Dynam Earthq Eng 2013;45:96–111.
[26] Chen ZX, Yang P, Liu HL, Zhang WG, Wu CZ. Characteristics analysis of granular landslide using shaking table model test. Soil Dynam Earthq Eng 2019;126. https://doi.org/10.1016/j.soildyn.2019.105761.
[27] Tamari Y, Towhata I. Seismic soil-structure interaction of cross sections of flexible underground structures subjected to soil liquefaction. Soils Found 2003;43(2):69–87.
[28] Wu Q, Ding XM, Chen ZX, Chen YM, Peng Y. Experimental study on seismic response of pile-soil-structure in coral sand under different earthquake intensity. Rock Soil Mech 2020;41(2):1–11. https://doi.org/10.16285/j.rsm.2019.0122. In this issue.